Egypt. J. Bot. **Vol. 63**, No. 3, pp. 1187-1199 (2023)

Egyptian Journal of Botany
http://ejbo.journals.ekb.eg/

Isolation, Identification, and Characterization of Extracellular Siderophore Triacetylfusarinine C (TafC) Produced by *Aspergillus fumigatus*

Marwa H. Azel[(1)], Sherif M. Sherif[(2)], Tarek A.A. Moussa[(3)#], Mohamed A. El-Desouky[(1)]

[(1)]Biochemistry Division, Faculty of Science, Cairo University, Giza 12613, Egypt;
[(2)]Chemistry Department, Faculty of Science, Cairo University, Giza 12613, Egypt;
[(3)]Botany and Microbiology Department, Faculty of Science, Cairo University, Giza 12613, Egypt.

HYDROXAMATE siderophores are low molecular weight, high-affinity ferric iron-chelating compounds which are excreted by *Aspergillus fumigatus* for iron transport extracellularly or iron storage intracellularly. *Aspergillus fumigatus* was isolated from different samples, then siderophores were extracted from *A. fumigatus* by phenol, and diethyl ether, and purified by amberlite XAD-16 resin. The chemical structure of siderophores was described by H^1NMR, ESI-MS/MS, and LC-MS/MS analysis. Also, antimicrobial activity was observed. From the elution profile of siderophores, the major peak was at fraction 28. As a result of H^1NMR analysis, the singlets assigned to the -C=O-CH=C (CH3) C-substructure were detected. The siderophore TafC had antibacterial activity against both G +ve and G -ve bacteria. Under different concentrations of iron, it can be deduced that the concentration of 0.03 mmol of iron at 20 hrs. incubation period was an ideal condition for mycelial fresh weight which positively affected, so production of siderophores increased. From chemical analysis, it was found that the chemical formula $C_{39}H_{58}FeN_6O_{15}$ was consistent with the known siderophore N, N', N"-triacetylfusarinine C (TafC).

Keywords: Antibacterial activity, *Aspergillus fumigatus*, ESI-MS/MS, 1H NMR, Hydroxamate siderophores, LC-MS/MS.

Introduction

Aspergillus fumigatus is an atypical saprophytic mold, which has become the most common airborne fungal pathogen of humans causing life-threatening invasive diseases, especially in immunocompromised patients such as organ transplant recipients and people with AIDS or leukemia (Schrettl et al., 2007). The fungus is more likely to be pathogenic, causing a range of diseases generally termed aspergillosis. The most common forms are allergic bronchopulmonary aspergillosis, pulmonary aspergilloma, and invasive forms of aspergillosis which cause fever, chills, shock, and blood clots. A person may develop kidney failure, liver failure, and death (Rokas et al., 2020).

Iron is required by living organisms for a variety of biochemical reactions in the cells. Most iron is found intracellularly in heme proteins and ferritin and iron outside cells are tightly bound to proteins (Ouf et al., 2023). *A. fumigatus* lack specific uptake systems for host iron sources. *A. fumigatus* employs two high–affinity iron uptake systems: reductive iron assimilation (RIA) and siderophores–assisted iron uptake, both are induced upon iron starvation (Schrettl et al., 2007; Kradin & Mark, 2008).

#Corresponding author email: tarekmoussa@yahoo.com
Received 13/06/2022; Accepted 21/08/2023
DOI: 10.21608/ejbo.2023.144429.2017
Edited by: Prof. Dr. Salama A. Ouf, Faculty of Science, Cairo University, Giza 12613, Egypt.

Siderophores are small, high–affinity iron-chelating compounds secreted by *A. fumigatus*. Siderophores are usually classified by the ligands used to chelate the ferric iron. The major groups of siderophores include catecholate, hydroxamates, and carboxylates (Kesaulya et al., 2018).

A. fumigatus produces three hydroxamate-type siderophores, extracellular fusarinine C (FSC) and triacetylfusarinine C (TafC), and intracellular ferricrocin (FC). The most prominent siderophore was identified as triacetylfusarinine C followed by ferricrocin, in addition to a hydrolytic product of triacetylfusarinine C. A novel siderophore was described, hydroxyferricrocin (HFC), employed for conidial iron storage (Schrettl et al., 2007; Aguiar et al., 2021). FSC and TafC mobilize extracellular conidial and hyphal iron storage. The hyphal siderophores ferricrocin plays an important role in intracellular iron distribution and iron storage. Conidial hydroxyferricrocin is of crucial importance for conidial iron storage (Schrettl et al., 2010).

This study aimed to search to produce siderophores from different strains of *Aspergillus fumigatus* and screen their production using different iron concentrations. Also, this work aimed to examine the chemical structure of selected siderophores by various chemical assays.

Materials and Methods

Isolation of Aspergillus fumigatus from different sources

Eight samples from different sources were used (Table 1), where the first four samples were taken from different regions in Kafr El-Sheikh Governorate, sample 5 from the atmosphere of New Cairo city, sample 6 from the mycology Lab. at Cairo University, sample 7 from the atmosphere of Cairo University and sample 8 from gardens at Cairo University. Soil samples were processed by two methods, soil dilution and soil plate methods on two different media named Potato Dextrose Agar (PDA) and Czapek's Dox (CZA) (Rebecca et al., 2013; Silambarasan & Abraham (2013). Samples were incubated at 37ºC for 5 days, then *Aspergillus fumigatus* was isolated.

Identification of Aspergillus fumigatus

Isolates of *A. fumigatus* were grown on specific media for identification: Malt Extract Agar (MEA), Czapek's Yeast Agar (CYA), and Czapek's Dox Agar (CZ) and incubated at 25˚C for seven days (Samson et al., 2004), then isolates were identified macroscopically and microscopically according to Nyongesa et al. (2015).

DNA preparation

To prepare samples for DNA extraction, isolates of *A. fumigatus* were grown on liquid Czapek's Dox medium with shaking at 120 rpm at 37ºC for 4 days, then mycelia were separated by filtration and were used as follows**:** to each sample, 500µL of extraction buffer was added according to Zhao et al. (2001).

PCR amplification and DNA sequencing

The most productive fungal isolate was identified using Internal Transcript Spacer (ITS). The fragments which contain ITS1 and ITS2 of the ribosomal DNA (rDNA) complex were amplified with primers ITS1, ITS2, ITS3, and ITS4 (ITS1: 5′-TCCGTAGGTGAACCTGCGG-3′; ITS2: 5′-GCTGCGTTCTTCATCGATGC-3′; ITS3: 5′-GCATCGATGAAGAACGCAGC-3′; ITS4, 5′-TCCTCCGCTTAT TGATATGC-3′). Primers ITS1, ITS2, ITS3, and ITS4 were used for sequencing amplification in both directions (Zhao et al., 2001).

TABLE 1. Samples from different sources (soil and air) [The first 4 samples were taken from different places in Kafr El-Sheikh Governorate, where symbols r1, r2, r3, and r4 refer to different regions]

Sample	Type	Source
1	Agricultural soil (**r1**)	Kafr El-Sheikh Governorate
2	Agricultural soil (**r2**)	Kafr El-Sheikh Governorate
3	Agricultural soil (**r3**)	Kafr El-Sheikh Governorate
4	Agricultural soil (**r4**)	Kafr El-Sheikh Governorate
5	Air	The atmosphere of New Cairo City
6	Air	Mycology Lab. at Cairo University
7	Air	The atmosphere of Cairo University
8	Soil	Gardens at Cairo University

Mycelial fresh weight

To screen the production of siderophores, minimal medium (MM) was used iron two conditions: iron-deplete condition (zero concentration of iron) and iron-replete condition (at concentrations of 0.03 and 0.5 mmol of iron) according to Alreshidi et al. (2019). For iron-replete conditions, $FeCl_3$ was added to the iron concentrations of 0.03mmol and 0.5mmol during the preparation of MM. Freshly prepared spore buffers were grown in each flask containing 100mL medium and were shaken at 200 rpm for 20 and 40h. at 37ºC, then the filtrate was obtained by filtration, and mycelia were used in fresh weight detection (Haas et al., 2011).

Siderophores determination

Free and bound hydroxylamine (hydroxamate siderophores) were estimated by using the Csaky method where samples were measured by spectrophotometer at 526nm (Ferreira et al., 2019).

Extraction of extracellular siderophores

Extracellular siderophores were extracted from filtrate with Phenol and diethyl ether (Haas et al., 2011). The aqueous phase (colored phase) concentration was measured by spectrophotometer at wavelength 440 nm using a molar extinction factor of 2996 ($M^{-1}cm^{-1}$). There is another method was used to measure triacetylfusarinine C (TafC) (an extracellular siderophore) concentration in the supernatant by using chloroform and diethyl ether, TafC was measured using a molar extinction factor of E = 2996 M^{-1} cm^{-1} at 440nm (Misslinger et al., 2018).

Purification of extracellular siderophores

$FeCl_3$ was added to the filtrate to a final concentration of 1.5mM to convert de-ferri siderophores to the ferri forms. These ferri forms were purified by using amberlite XAD-16 resin (CWG) according to Oberegger et al. (2001) and were eluted with methanol. Fractions were collected at equal volumes (1mL for each fraction) and extracellular siderophores were measured photometrically at 435nm.

Chemical characterization of extracellular siderophore (TafC)

Proton nuclear magnetic resonance (^{1}H NMR) analysis

The ^{1}H NMR spectrum of the purified siderophores was collected on an Inova 600 Mhz NMR spectrophotometer equipped with a triplet resonance probe and triple-axis gradients (Murugappan et al., 2011).

Electrospray ionization-Mass spectrometry/ Mass spectrometry (ESI-MS/MS) analysis

Metal–ligand complex was analyzed in an ion trap MS instrument which involved a high-resolution electrospray ionization (ESI) and coupled Orbitrap Elite Mass spectrometer. The analyzer of Orbitrap mass was operated in positive ionization mode (Tsednee et al., 2016).

Liquid chromatography- Mass spectrometry/ Mass spectrometry (LC-MS/MS) analysis

LC-MS/MS analysis was performed where separation of TafC was done using the reverse phase C18 column (Li et al., 2012).

Antimicrobial activity of TafC siderophore

The antimicrobial activity of the tested isolates was determined using a modified Kirby-Bauer disc diffusion method (Erum et al., 2015). Strains used in the work were divided into 3 groups: Gram-positive and Gram-negative and fungi (yeast-like and filamentous).

Results

Isolation and identification of Aspergillus fumigates

Eight samples from different sources (soils and air) were cultured to isolate *Aspergillus* spp. and result in 26 fungal *Aspergillus* spp. distributed as 4 isolates from each of samples 1, 2, and 4; 3 isolates from sample 3; 2 isolates from each sample 5, 6, and 7, and finally 5 isolates from sample 8. Seven *Aspergillus* species were isolated from the eight samples as shown in Table 2.

The *A. fumigatus* isolate was identified on a molecular level using ITS. The isolates showed high identity with the *A. fumigatus* (KM582649). The sequence of the ITS region for the *A. fumigatus* was done and it has a partial sequence of 766 bp. The main structure of the sequence was 18S rRNA. The phylogenetic relationship between the intended *A. fumigatus* isolates and the *A. fumigatus* (KM582649), *A. flavus* MT680658, and *A. oryzae* MT680659 deposited in the gene database. The results revealed that the intended isolate was very related to that in database *A. fumigatus* (KM582649) as shown in Figs. 1 and 2.

TABLE 2. Isolation and identification of the isolates which resulted from different sources

Sample code*	Type of sample	Location	Isolates
1A	Agricultural soil **(r1)**	Kafr El-Sheikh Governorate	*Aspergillus flavus*
1B			*Aspergillus fumigatus*
1C			*Aspergillus terreus*
1D			*Aspergillus clavatus*
2A	Agricultural soil **(r2)**	Kafr El-Sheikh Governorate	*Aspergillus terreus*
2B			*Aspergillus flavus*
2C			*Aspergillus fumigatus*
2D			*Aspergillus niger*
3A	Agricultural soil **(r3)**	Kafr El-Sheikh Governorate	*Aspergillus fumigatus*
3B			*Aspergillus niger*
3C			*Aspergillus ochraceus*
4A	Agricultural soil **(r4)**	Kafr El-Sheikh Governorate	*Aspergillus fumigatus*
4B			*Aspergillus flavus*
4C			*Aspergillus niger*
4D			*Aspergillus nidulans*
5A	Air	Atmosphere, New Cairo city	*Aspergillus niger*
5B			*Aspergillus fumigatus*
6A	Air	Mycology Lab., Cairo University	*Aspergillus ochraceus*
6B			*Aspergillus fumigatus*
7A	Air	Atmosphere, Cairo University	*Aspergillus fumigatus*
7B			*Aspergillus niger*
8A	Soil	Gardens, Cairo University	*Aspergillus fumigatus*
8B			*Aspergillus niger*
8C			*Aspergillus clavatus*
8D			*Aspergillus ochraceus*
8E			*Aspergillus terreus*

*Sample Code: r1, r2, r3, r4 refer to different regions in Kafr El-Sheikh Governorate.

```
1 TTAGCATGGG ATAATGGAAT AGGACGTGCG GTTCTATTTT GTTGGTTTCT AGGACCGCCG   60
61 TAATGATTAA TAGGGATAGT CGGGGGCGTC AGTATTCAGC TGTCAGAGGT GAAATTCTTG  120
121 GATTTGCTGA AGACTAACTA CTGCGAAAGC ATTCGCCAAG GATGTTTTCA TTAATCAGGG 180
181 AACGAAAGTT AGGGGATCGA AGACGATCAG ATACCGTCGT AGTCTTAACC ATAAACTATG 240
241 CCGACTAGGG ATCGGGCGGT GTTTCTATTA TGACCCGCTC GGCACCTTAC GAGAAATCAA 300
301 AGTTTTTGGG TTCTGGGGGG AGTATGGTCG CAAGGCTGAA ACTTAAAGAA ATTGACGGAA 360
361 GGGCACCACA AGGCGTGGAG CCTGCGGCTT ACTTTGACTC AACACGGGGA AACTCACCAT 420
421 GTCCAGACAA AATAAGGATT GACAGATTGA GAGCTCTTTC TTTATCTTTT GGATGGTGGT 480
481 GCATGGCCGC TCTTAGTTGG TGGAGTGATT TGTCTTCTTA ATTGCGATAA CGAACGAGAC 540
541 CTCGGCCCTT AAATAGCCCG GTCCGCAGTT GCGGGCCGCT GGCTTCTTAG GGGGACTATC 600
601 GGCTCAAGCC GATGGAAGTG CGCGGCAATA ACAGGTCTGT GATGCCCTTA GATGTTCTGG 660
661 GCCGCACGCG CGCTACACTG ACAGGGCCAG CGAGTACTTC ACCTTGGCCG AGAGGTCTGG 720
721 GTAATCTTGT TAAACCCTAT CGTGCGGGGG ATAGAGCATT GCAATA 766
```

Fig. 1. Partial sequence of ITS region of the fungal isolate *A. fumigatus* showing 18S rRNA

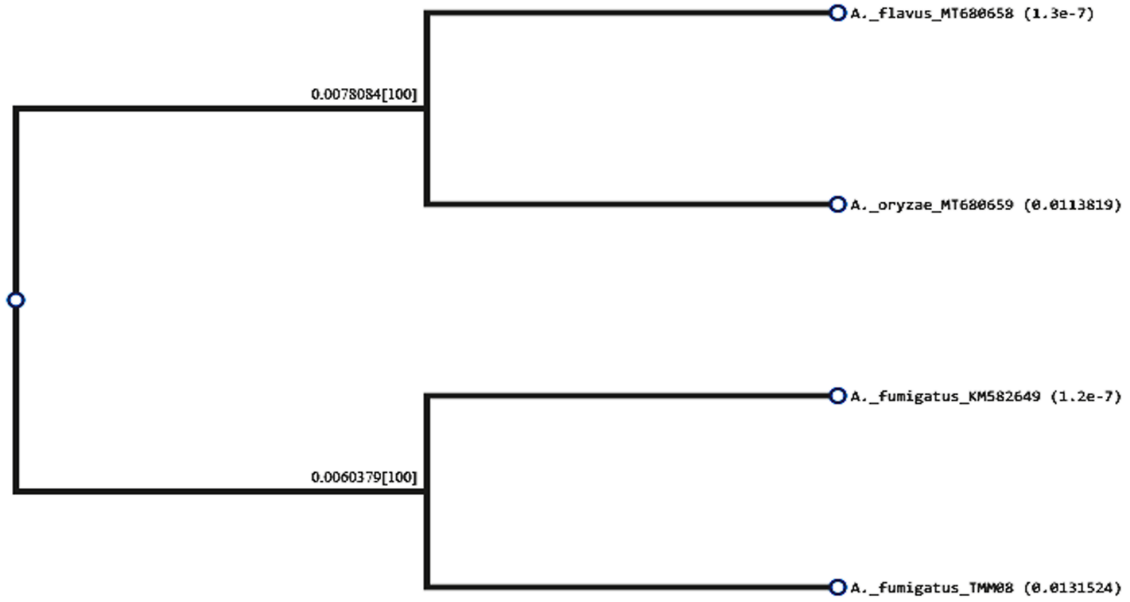

Fig. 2. Phylogenetic tree of the *A. fumigatus* TMM08 with another *Aspergillus* spp. in the database (*A. fumigatus* KM582649, *A. flavus* MT680658, and *A. oryzae* MT680659)

Mycelial Fresh weight

After 20 hrs of incubation, the results showed that *A. fumigatus* isolate 8A was the highest production of mycelia under iron-depleted conditions, while isolate 7A was the highest production of mycelia under iron repleted conditions. After 40h. of incubation, isolates 8A and 3A were the highest production of mycelia in the absence and presence of iron, while isolate 1B showed a remarkable increase in mycelial fresh weight under iron conditions. The addition of iron with 0.03 and 0.5mmol had a little difference in the fresh weight of *A. fumigatus*. (Table 3).

Determination and extraction of extracellular siderophores

According to the Csaky method, isolate (8A) has the highest absorbance in the extracellular siderophores (filtrate) followed by isolate (7A) while the lowest absorbance was in isolate 3A) (Table 4 and Fig. 3), but in the case of extraction of filtrate (resulted from 20h. incubation) with phenol and diethyl ether, isolate 3A was highest in concentration while the lowest was isolate 1B (Fig. 4).

TABLE 3. Mycelial fresh weight (g/100 ml) of different A. fumigatus isolates using different iron concentration supplements after 20 h and 40 h incubation

Isolate No.	Iron supplementation (mmol)					
	0		0.03		0.5	
	20h	40h	20h	40h	20h	40h
1B	0.82	4.96	7.16	7.06	6.13	7.87
2C	2.59	4.34	4.59	6.17	4.66	6.89
3A	3.39	6.2	6.23	8.82	5.79	8.84
4A	1.782	3.72	4.41	5.29	4.36	5.89
5B	2.03	4.48	3.74	4.57	3.47	4.61
6B	2.07	4.03	3.67	5.73	3.72	6.39
7A	2.97	5.37	7.35	5.48	7.26	5.53
8A	3.7	8.95	6.35	9.14	6.65	9.22

TABLE 4. Csaky method for detection of extracellular siderophores

Isolate number	Absorbance
1B	0.074
2C	0.062
3A	0.020
4A	0.026
5B	0.028
6B	0.027
7A	0.185
8A	0.376

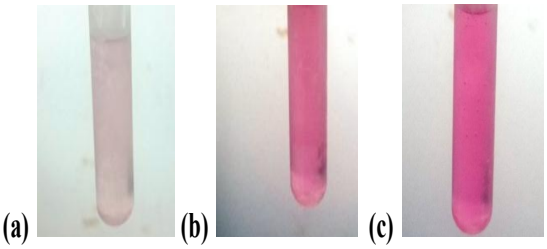

Fig. 3. Color development of extracellular siderophore in Csaky method (a) control, (b) Isolate 7A, and (c) Isolate 8A

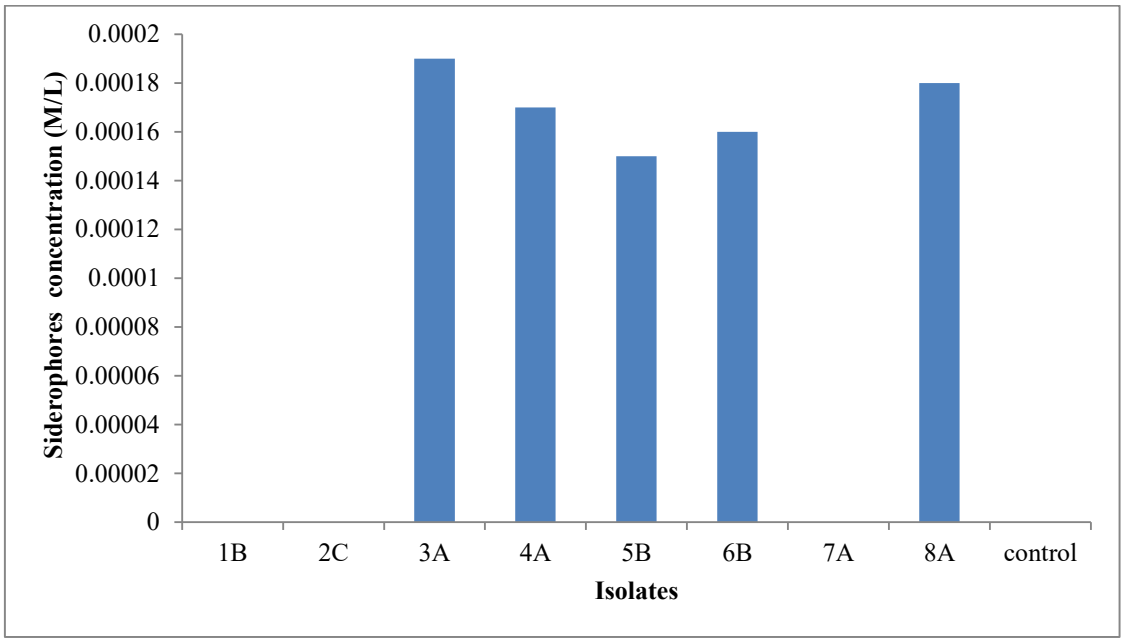

Fig. 4. Quantification of the extracted extracellular siderophores from *A. fumigatus*

As a result of extraction with chloroform and diethyl ether, isolate 8A was the highest concentration of TafC while isolate 5B was the lowest, in both chloroform and aqueous phases and in the absence of iron. Isolate 1B was the highest in concentration while isolates 4A and 5B were the lowest, in the aqueous phase, at a concentration (0.03mmol) of iron (Table 5).

Purification of extracellular siderophores (TafC)

Figure 5 showed the elution profile of the extracellular siderophores (TafC). From the profile, the major peak was at fractions 27-29 with a maximum at fraction 28 (absorbance 0.98). In this study, the chemical nature of the extracellular siderophore N, N', N"-triacetylfusarinine C was examined by different techniques as follows.

^{1}H NMR analysis

Purified TafC was quantified by absorbance (ε440= 2960M^{-1} cm^{-1}). The singlets at 6.3 and 1.86 ppm which can be assigned to the -C=O-CH=C(CH3)-C-substructure were detected. The singlet at 1.83 ppm corresponds to the methyl protons of the acetyl group(s) (Fig. 6).

ESI-MS/MS analysis

The major peak detected with the iron isotope pattern had an m/z of 906.3304 which has an isotopic profile that matches the formula $C_{39}H_{58}FeN_6O_{15}$ (Fig. 7) and Screening of iron-containing compound in the fungal extract revealed this to be the only that was detected. The iron-chelated metabolite was detected in *A. fumigatus* TMM08 isolate that was identified as virulent.

TABLE 5. Production of extracellular siderophore triacetylfusarinine C (TafC) of different *Aspergillus fumigatus* isolates using different iron concentration supplements after 20h of incubation

Isolate no.	Chloroform (O.D.±S.D.)			Aqueous (O.D.±S.D.)		
	Iron supplementation (mmol)					
	0	0.03	0.5	0	0.03	0.5
1B	0.23±0.003	0.0±0.0	0.0±0.0	0.18±0.004	0.047±0.001	0.0±0.0
2C	0.29±0.003	0.0±0.0	0.0±0.0	0.16±0.002	0.012±0.00	0.0±0.0
3A	0.24±0.003	0.0±0.0	0.0±0.0	0.13±0.002	0.011±0.00	0.0±0.0
4A	0.28±0.002	0.0±0.0	0.0±0.0	0.15±0.0007	0.010±0.00	0.0±0.0
5B	0.17±0.004	0.0±0.0	0.0±0.0	0.092±0.0007	0.010±0.00	0.0±0.0
6B	0.198±0.002	0.0±0.0	0.0±0.0	0.386±0.002	0.017±0.00	0.0±0.0
7A	0.87±0.003	0.0±0.0	0.0±0.0	0.42±0.004	0.015±0.001	0.0±0.0
8A	0.94±0.0007	0.0±0.0	0.0±0.0	0.50±0.006	0.0185±0.0007	0.0±0.0

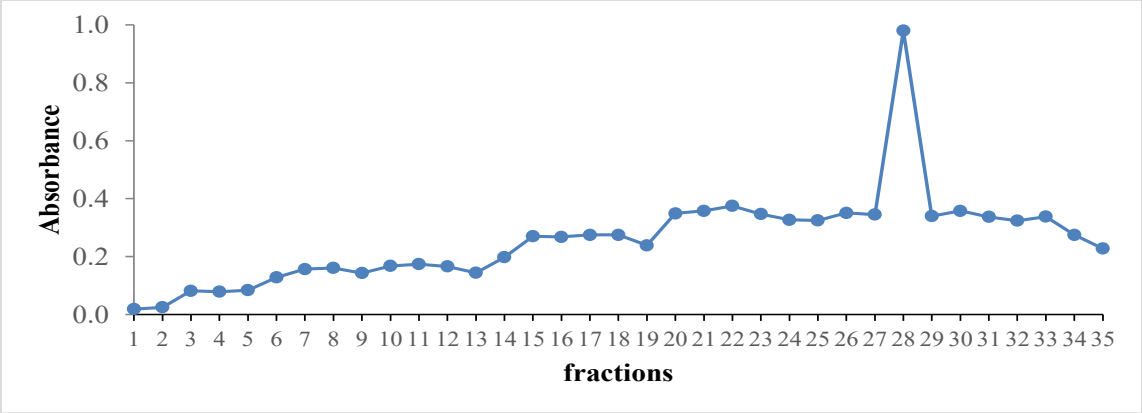

Fig. 5. The elution profile of the extracellular siderophore extracted from the culture filtrate of *A. fumigatus* using methanol as a mobile phase

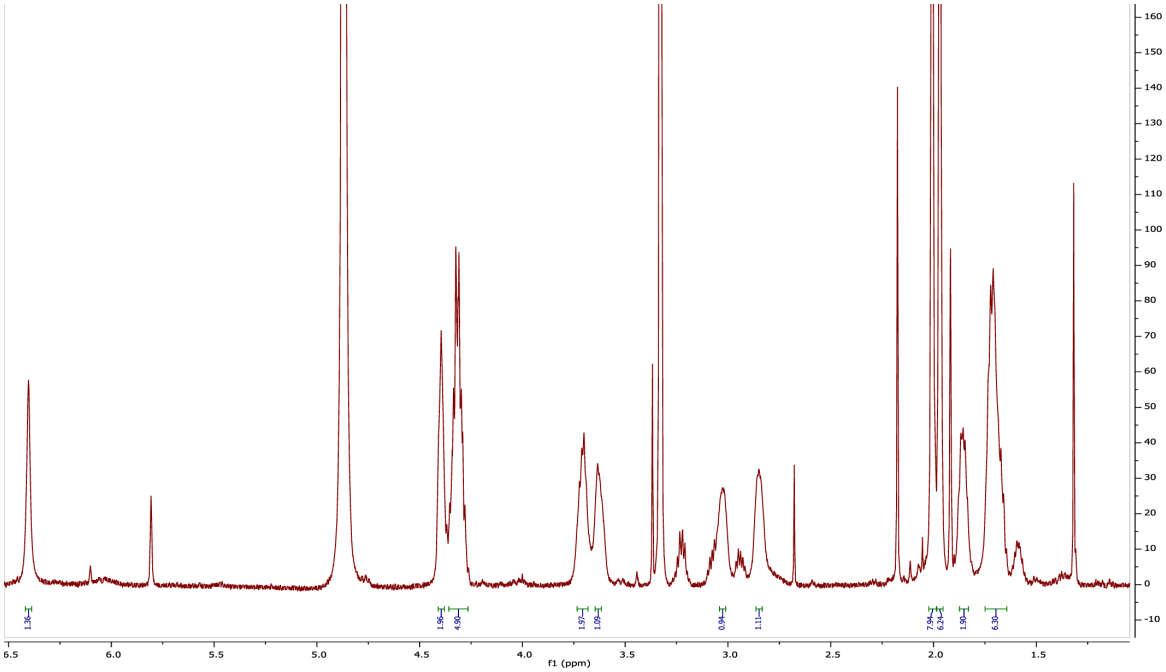

Fig. 6. NMR Spectra and Peak assignments of N, N', N''-Triacetylfusarinine C taken in CD3OD on an Inova 600Mhz NMR [The doublet at 4.4 ppm with a coupling constant of 6.0Hz can be assigned to the -NH-CH2 group]

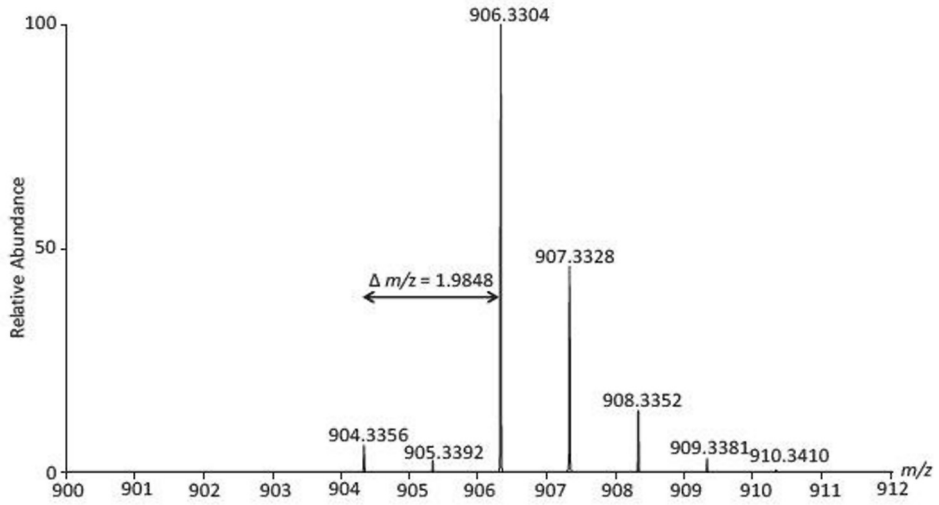

Fig. 7. Positive mode ESI pattern of [M+H] ion of $C_{39}H_{58}FeN_6O_{15}$, which shows the unique pattern indicating the presence of Fe, Isolation, and identification of N, N', N"-triacetylfusarinine C as a predominant siderophore of *A. fumigatus*

LC-MS/MS analysis

Examination of the nonchelated precursor ion's MS/MS fragmentation pattern at m/z 853.4123 revealed two neutral losses of 284.135 Da, leaving a product with an m/z of 285.1421. (Fig. 8).

Antimicrobial activity of the extracellular siderophore TafC

The results in Table 6 showed that the siderophore TafC had antibacterial activity against both G +ve and G -ve bacteria whereas *S. aureus* was more susceptible to TafC in G +ve and *P. aeruginosa* was more susceptible to TafC in G -ve bacteria. The antifungal activity of TafC against *A. flavus* and *C. albicans* showed no activity which may be due to its fungal origin. The antifungal antibiotic amphotericin B showed considerable activity against the two fungal species used.

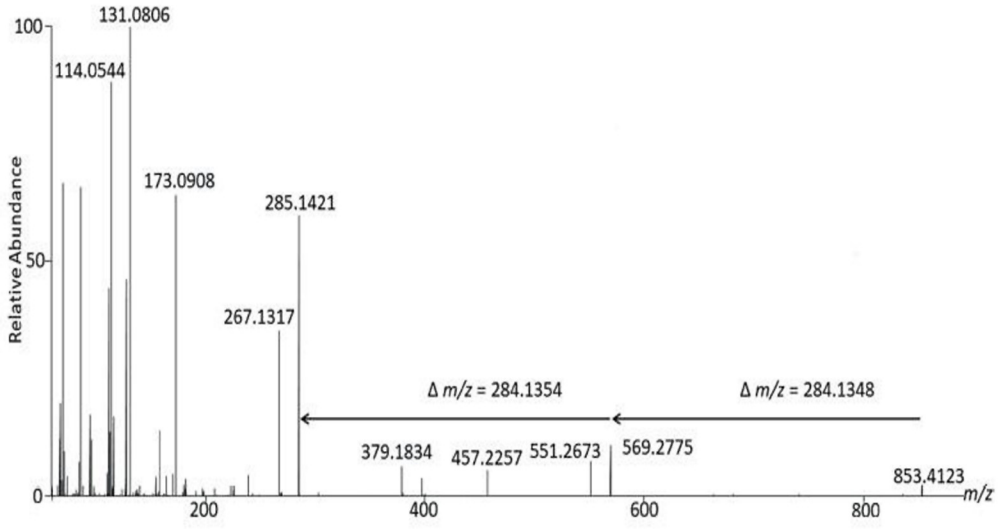

Fig. 8. MS/MS of unbound N, N', N"-triacetylfusarinine C. Stepped 25/55 NCE MS/MS spectra of unbound N, N', N"-triacetylfusarinine C [Diagnostic product ions of an m/z of 285.1421 and 569.2775. NCE, normalized collision energy]

TABLE 6. Antibacterial activity of the extracellular siderophore TafC

Sample	Inhibition zone diameter (mm)			
	Gram-Positive		Gram-Negative	
	Bacillus subtilis	*Staphylococcus aureus*	*Escherichia coli*	*Pseudomonas aeruginosa*
Ampicillin (10µg/mL)	26	21	25	26
TafC (10µg/mL)	9	10	9	10

Discussion

The soil is a rich habitat for the growth of microorganisms more than any other microbial habitat. Among these microorganisms, fungi are one of the dominant groups present in the soil, which represents the main reservoir of fungi (Rane & Gandhe, 2006). In this work, samples from different sources (soils and air) were cultured to isolate *Aspergillus* spp. and result in 26 fungal *Aspergillus* spp. *Aspergillus* isolates were selected in each sample according to matching the distinguishing characteristics of *Aspergillus* spp.

As a result of identification, it was found that 7 *Aspergillus* species were isolated from the eight samples. *Aspergillus fumigatus* followed by *Aspergillus niger* is the most distributed and where *Aspergillus fumigatus* was found in all isolated samples, but Gautier et al. (2016) show different results wherein *Aspergillus fumigatus* followed by *Aspergillus flavus* are the most frequent species involved in human disease.

In this work, the *A. fumigatus* isolate was identified on a molecular level using ITS. The results revealed that the intended isolate was very related to that in database *A. fumigatus* (KM582649) because all *Aspergillus* species have the specified sequence of ITS region which is used in molecular identification and this matched with Diba et al. (2019) which he shows that forward and reverse primers were used to amplify *Aspergillus* ITS regions and amplified ITS fragments of *Aspergillus* sp. were checked by using agarose gel electrophoresis where all species make the same size PCR bands.

In this work, after incubation for 20, 40h. and shaking with 200 rpm at 37ºC, it was obvious from the experimental results that nearly all *Aspergillus fumigatus* isolates used in this study manifested more growth as fresh mycelia weight under a scarcity of iron (0.03mmol) than in case of its complete absence regardless of incubation time. The addition of iron with 0.03 and 0.5mmol had a little difference on the fresh weight of *A. fumigatus*, so the concentration of 0.03 mmol of iron at 20h. only was used in the next experiments, also these conditions were ideal for the growth of fungi and subsequently effect on fresh weight mycelia were, fresh weight directly proportional to increase in iron concentration(0 and 0.03mmol), these results matched with Wiemann et al. (2014) who show that addition of different concentrations of iron in for 24h. at 37°C at 250 rpm cause increase in dry weight of *A. fumigatus*. Also, Baldin et al. (2015) proved that dry mycelial weight of *A. fumigatus* in the case of iron-replete liquid medium (medium contained 30µM $FeSO_4$) at 37◦C for 16h. is higher than dry mycelial weight (g) in case of iron-depleted conditions (medium contained 0µM $FeSO_4$) at the same conditions.

In this study, the Csaky method was used to estimate free and bound hydroxylamine (hydroxamate siderophores). Based on the Csaky method results, it seemed that *A. fumigatus* isolates used in this study were capable to synthesize hydroxamate siderophores and producing both extracellular and intracellular siderophores, but they all produced more amounts of intracellular siderophores. This study was compatible with Khan et al. (2017) who found that *A. fumigatus* produces two extracellular fusarinine-type siderophores as well as two intracellular ferrichrome-type siderophores. Also, Chowdappa et al. (2020) indicate the production of hydroxamate siderophores by endophytic fungi by using the Csaky assay which recorded the presence of hydroxamate type of siderophore by the development of deep pink color.

In this work, extracellular siderophores were extracted with phenol and diethyl ether, and siderophores concentration was measured by spectrophotometer at wavelength 440 nm using a molar extinction factor of 2996 (M^{-1}, cm^{-1}).

This work matched with Osman et al. (2019) who showed that the extraction of hydroxamate siderophores from *Aspergillus niger* was take place by using phenol-chloroform and diethyl ether, but not matched with Patil et al. (2021) which revealed that hydroxamate siderophores from different *A. fumigatus* strains were extracted with ethyl acetate and methanol. As well, in this work, triacetylfusarinine C (TafC) was extracted with chloroform and diethyl ether under the same conditions as above, and these results matched with Pahlow et al. (2020) who revealed that extraction of TAFC took place by addition of a 1:1 mixture of chloroform and diethyl ether.

At present work, siderophores were purified from culture supernatants by XAD-16 resin and this work was compatible with Wu et al. (2021) who showed that siderophores were purified from filtrates of fungal strains by Amberlite XAD-16 resins but was incompatible with Maglangit et al. (2019) where they showed that siderophores were purified by reversed-phase C18 High-Performance Liquid Chromatography (HPLC).

In this study, the chemical nature of the extracellular siderophore N, N', N"-triacetylfusarinine C was determined by different analyses such as ^{1}H NMR where the isolated compound was confirmed by comparison to previously acquired spectra of TafC and ESI-MS/MS analysis in which the chemical formula $C_{39}H_{58}FeN_6O_{15}$ was consistent with the known siderophore N, N', N"-triacetylfusarinine C (TafC) and finally LC-MS/MS analysis was used to characterize the chemical structure. This study matched with Kügler et al. (2020) who characterized a novel siderophore produced from the bacterium *Pseudomonas* species by NMR analysis, also matched with Acquah et al. (2020) who show those hydroxamate siderophores produced by Actinomycete *Kribbella speibonae* SK5 were characterized by High Resonance Electrospray ionization-Mass spectrometry (HRESIMS) (positive mode). In addition to that, Jarmusch et al. (2021) revealed that high-resolution LC-MS/MS was used for the structure elucidation of hydroxamate siderophores produced from *Streptomyces* spp. S29.

In the present study, the antimicrobial activity of the extracellular siderophore TafC was carried out using inhibition zone diameter and results showed that TafC had antibacterial activity, these results matched with Chowdappa et al. (2020) who revealed that the antibacterial activity of siderophores produced by Endophytic fungi was determined by a disc diffusion assay where the results proved that the siderophore exhibited the highest zone of inhibition on plant pathogens. Essential oils have been used as antifungal agents against *A. fumigatus* (Abd El-Zaher et al., 2019).

Conclusion

From molecular identification, it was concluded that the intended isolate was very related to *A. fumigatus* (KM582649) which is present in the database. It can be deduced that the fresh weight of mycelia increased at a concentration of 0.03 mmol of iron and 20 hrs. incubation period, subsequently, consequently, the production of siderophores increased. From chemical analysis, it was found that the chemical formula $C_{39}H_{58}FeN_6O_{15}$ was consistent with the known siderophore N, N', N"-triacetylfusarinine C (TafC). It was revealed that TafC had antibacterial activity against both G +ve and G -ve bacteria.

Conflict of interest: The authors confirm that they have no competing interests.

Authors' contributions: TAAM conceptualization the idea; MHA methodology; TAAM, SMS and MAE supervision; TAAM, MHA and MAE data curation; TAAM validation and investigation; MAE and MHA writing the manuscript; TAAM edit and review the manuscript.

Ethics approval: Not applicable.

References

Abd El-Zaher, E.H.F., El-Shouny, W.A., Shabana, S.A., Abd El-Salam, O. (2019) Efficiency of essential oils as antifungal agents against *Aspergillus fumigatus* KY026061 causing allergic bronchopulmonary aspergillosis (ABPA). *Egyptian Journal of Botany*, **59,** 595-604.

Acquah, K.S., Beukes, D.R., Warner, D.F., Meyers, P.R., Sunassee, S.N., Maglangit, F., et al. (2020) Novel South African rare actinomycete *Kribbella speibonae* strain SK5: A prolific producer of hydroxamate siderophores including new dehydroxylated congeners. *Molecules,* **25**, 2979. http://doi.org/10.3390/molecules25132979.

Aguiar, M., Orasch, T., Misslinger, M., Dietl, A.-M., Gsaller, F., Haas, H. (2021) The siderophore transporters *Sit*1 and *Sit*2 are essential for utilization of ferrichrome-, ferrioxamine- and coprogen-type siderophores in *Aspergillus fumigatus*. *Journal of Fungi,* **7,** 768. https://doi.org/10.3390/jof7090768.

Alreshidi, M.M., Dunstan, R.H., Macdonald, M.M., Smith, N.D., Gottfries, J., Roberts, T.K. (2019) Amino acids and proteomic acclimation of *Staphylococcus aureus* when incubated in a defined minimal medium supplemented with 5% sodium chloride. *Microbiology Open,* **8**, e00772. http://doi.org/10.1002/mbo3.772.

Baldin, C., Valiante, V., Krüger, T., Schafferer, L., Haas, H., Kniemeyer, O., Brakhage, A.A. (2015) Comparative proteomics of a tor inducible *Aspergillus fumigatus* mutant reveals involvement of the Tor kinase in iron regulation. *Proteomics,* **15**, 2230–2243.

Chowdappa, S., Jagannath, S., Konappa, N., Udayashankar, A.C., Jogaiah, S. (2020) Detection and characterization of antibacterial siderophores secreted by endophytic fungi from *Cymbidium aloifolium*. *Biomolecule,* **10,** 1412. http://doi.org/0.3390/biom10101412.

Diba, K., Jangi, F., Makhdoomi, K., Moshiri, N., Mansouri, F. (2019) *Aspergillus* diversity in the environments of nosocomial infection cases at a university hospital. *Journal of Medicine and Life,* **12,** 128-132.

Erum, A., Bashir, S., Saghir, S. (2015) Modified and unmodified arabinoxylans from *Plantago ovata* husk: Novel excipients with antimicrobial potential. *Bangladesh Journal of Pharmacology,* **10**, 765-769.

Ferreira, C.M.H., Vilas-Boas, Â., Sousa, C.A., Soares, H.M., Soares, E.V. (2019) Comparison of five bacterial strains producing siderophores with ability to chelate iron under alkaline conditions. *AMB Express,* **9**, 78. https://doi.org/10.1186/s13568-019-0796-3.

Gautier, M., Normand, A.-C., Ranque, S. (2016) Previously unknown species of *Aspergillus*. *Clinical Microbiology and Infection,* **22**, 662-669.

Haas, H., Blatzer, M., Binder, U. (2011) The metalloreductase *FreB* is involved in adaptation of *Aspergillus fumigatus* to iron starvation. *Fungal Genetics and Biology,* **48**, 1027–1033.

Jarmusch, S.A., Susaeta, D.L., Diab, E., Salazar, O., Asenjo, J.A., Ebela, R., Jaspar, M. (2021) Iron-meditated fungal starvation by lupine rhizosphere-associated and extremotolerant *Streptomyces* sp. S29 desferrioxamine production. *Molecular Omics,* **17**, 95-107.

Kesaulya, H., Hasinu, J.V., Tuhumury, G.N. (2018) Potential of *Bacillus* spp. produces siderophores in suppressing the wilt disease of banana plants. In: *IOP* Conf. Ser.*: Earth and Environmental Science,* **102,** 012-016. IOP Publishing.

Khan, A., Singh, P., Srivastava, A. (2017) Synthesis, nature and utility of universal iron chelator-siderophore: A review. *Microbiological Research,* **212-213**, 103–111.

Kradin, R., Mark, E.J. (2008) The pathology of pulmonary disorders due to *Aspergillus* spp. *Archives of Pathology and Laboratory Medicine,* **132**, 606-614.

Kügler, S., Cooper, R.E., Boessneck, J., Küsel, K., Wichard, T. (2020) Rhizobactin B is the preferred siderophore by a novel *Pseudomonas* isolate to obtain iron from dissolved organic matter in peatlands. *Biometals,* **33**, 415–433.

Li, H., Ortiz, R., Tran, L., Hall, M., Spahr, C., Walker, K., Laudemann, J., Miller, S., Moosavi, H.S., Lee, J.W. (2012) General LC-MS/MS method approach to quantify therapeutic monoclonal antibodies using a common whole antibody internal standard with application to preclinical studies. *Analytical Chemistry,* **84**, 1267-1273.

Maglangit, F., Tong, M.H., Jaspars, M., Kyeremeh, K., Deng, H. (2019) Legonoxamines A-B, two new hydroxamate siderophores from the soil bacterium, *Streptomyces sp*. MA37. *Tetrahedron Letters,* **60**, 75–79.

Misslinger, M., Lechner, B.E., Bacher, K., Haas, H. (2018) Iron-sensing is governed by mitochondrial, not by cytosolic iron-sulfur cluster biogenesis in *Aspergillus fumigatus*. *Metallomics,* **10**, 1687-1700.

Murugappan, R.M., Aravinth, A., Karthikeyan, M. (2011) Chemical and structural characterization of hydroxamate siderophore produced by marine

Vibrio harveyi. *Journal Industrial Microbiology and Biotechnology,* **38**, 265–273.

Nyongesa, B.W., Okoth, S., Ayugi, V. (2015) Identification key for *Aspergillus* species isolated from maize and soil of Nandi County, Kenya. *Advances in Microbiology,* **5**, 205-229.

Oberegger, H., Schoeser, M., Zadra, I., Abt, B., Haas, H. (2001) SREA is involved in regulation of siderophore biosynthesis, utilization and uptake in *Aspergillus nidulans*. *Molecular Microbiology,* **41**, 1077–1089.

Osman, Y., Gebreil, A., Mowafy, A.M., Anan, T.I., Hamed, S.M. (2019) Characterization of *Aspergillus niger* siderophore that mediates bioleaching of rare earth elements from phosphorites. *World Journal of Microbiology and Biotechnology,* **35**, 93. https://doi.org/10.1007/s11274-019-2666-1.

Ouf, S., El-Amriti, F., Abu-Elghait, M., Desouky, S., Mohamed, M. (2023) Role of plant growth promoting Rhizobacteria in healthy and sustainable agriculture. *Egyptian Journal of Botany,* **63**(2), 333-359. http://doi: 10.21608/ejbo.2023.191783.2246.

Pahlow, S., Orasch, T., Žukovskaja, O., Bocklitz, T., Haas, H., Weber, K. (2020) Rapid detection of the aspergillosis biomarker triacetylfusarinine C using interference-enhanced Raman spectroscopy. *Analytical and Bioanalytical Chemistry,* **412**, 6351–6360.

Patil, R.H., Kotta-Loizou, I., Palyzová, A., Pluháček, T., Coutts, R.H.A., Stevens, D.A., Havlíček, V. (2021) Freeing *Aspergillus fumigatus* of polymycovirus infection renders it more resistant to competition with *Pseudomonas aeruginosa* due to altered iron-acquiring tactics. *Journal of Fungi,* **7**, 497. https://doi.org/10.3390/jof7070497.

Rane, G., Gandhe, R.V. (2006) Seasonal distribution of soil fungi from forest soils of Jalgaon district, Maharashtra. *Zoos' Print Journal,* **21**, 2407-2409.

Rebecca, L.J., Susithra, G., Sharmila, S., Das, M.P. (2013) Isolation and screening of chitinase producing *Serratia marcescens* from soil. *Journal of Chemical and Pharmaceutical Research,* **5**, 192-195.

Rokas, A., Mead, M.E., Steenwyk, J.L., Oberlies, N.H., Goldman, G.H. (2020) Evolving moldy murderers: *Aspergillus* section *Fumigati* as a model for studying the repeated evolution of fungal pathogenicity. *PLoS Pathogens,* **16**, e1008315. https://doi.org/10.1371/journal.ppat.1008315.

Samson, R.A., Hoekstra, E.S., Frisvad, J.C. (2004) "*Introduction to Food and Airborne Fungi*". 7th ed, Centraalbureau voor Schimmelcultures, Utrecht

Schrettl, M., Bignell, E., Kragl, C., Sabiha, Y., Loss, O., Eisendle, M., Wallner, A., Arst, H.N.Jr., Haynes, K., Haas, H. (2007) Distinct roles for intra- and extracellular siderophores during *Aspergillus fumigatus* infection. *PLoS Pathogens,* **3**, e128. http://doi.org/10.1371/journal.ppat.0030128.

Schrettl, M., Ibrahim, M., Drive, S., Huerre, M., Large, J.-P., Haas, H. (2010) The crucial role of the *A. fumigatus* siderophore system in interaction with alveolar macrophages. *Microbial Infection,* **12**, 1035-1044.

Silambarasan, S., Abraham, J. (2013) Ecofriendly method for bioremediation of chlorpyrifos from agricultural soil by novel fungus *Aspergillus terreus* JAS1. *Water, Air and Soil Pollution,* **224**, 1-11.

Tsednee, M., Huang, Y.C., Chen, Y.R., Yeh, K.C. (2016) Identification of metal species by ESI-MS/MS through release of free metals from the corresponding metal-ligand complexes. *Scientific Report*, **6**, 26785. https://doi.org/10.1038/srep26785.

Wiemann, P., Lechner, B.E., Baccile, J.A., Velk, T.A., Yin, W.B., Bok, J.W., et al. (2014) Perturbations in small molecule synthesis uncovers an iron-responsive secondary metabolite network in *Aspergillus fumigatus*. *Frontiers in Microbiology,* **5**, 530. https://doi.org/10.3389/fmicb.2014.00530.

Wu, P.-C., Chen, Y.-K., Yago, J.I., Chung, K.R. (2021) Peroxisomes implicated in the biosynthesis of siderophores and biotin, cell wall integrity, autophagy, and response to hydrogen peroxide in the citrus pathogenic fungus *Alternaria alternate*. *Frontiers in Microbiology*, **12**, 645792. http://doi.org/10.3389/fmicb.2021.645792.

Zhao, J., Kong, F., Li, R., Wang, X., Wan, Z., Wang, D. (2001) Identification of *Aspergillus fumigatus* and related species by nested PCR targeting ribosomal DNA internal transcribed spacer regions. *Journal of Clinical Microbiology*, **39,** 2261–2266.

عزل وتعريف وتوصيف حامل الحديد ترايستيل فيوزارنين سى والمفرز خارج الخلية والمنتج بواسطة الأسبرجيللس فيومجاتس

مروة حسنى عازل[1]، شريف مراد شريف[2]، طارق عبدالموجود عبدالمطلب موسى[3]، محمد على الدسوقى[1]
[1]شعبة الكيمياء الحيوية- قسم الكيمياء- كلية العلوم- جامعة القاهرة- الجيزة 12613- مصر، [2]قسم الكيمياء- كلية العلوم- جامعة القاهرة- الجيزة 12613- مصر، [3]قسم النبات والميكروبيولوجى- كلية العلوم، جامعة القاهرة، الجيزة 12613- مصر.

حاملات حديد هيدروكسيميت هي عبارة عن مركبات مخلبة لأيونات الحديديك منخفضة الوزن الجزيئي وعالية الألفة تفرز بواسطة الاسبرجيللس فيومجاتس لنقل الحديد خارج الخلية أو تخزين الحديد داخل الخلايا. تم عزل الاسبرجيللس فيومجاتس من عينات مختلفة، ثم تم استخلاص حامل الحديد من الاسبرجيللس فيومجاتس بواسطة الفينول، وثنائي إيثيل إيثر، وتنقيته بواسطة راتينج الأمبرلايت XAD-16. تم توصف التركيب الكيميائي لحامل الحديد بواسطة تحليل H^1NMR وESI-MS/MS وLC-MS/MS. كما لوحظ نشاط مضادات الميكروبات. أظهرت التنقية والفصل لحامل الحديد، كانت الذروة الرئيسية عند العينة رقم 28. ونتيجة لتحليل H^1NMR، تم اكتشاف المفردات المخصصة للبنية التحتية C -C=O-CH=C (CH3). كان لمركب Siderophore TafC نشاط مضاد للجراثيم ضد كل من بكتيريا G + ve وG -ve. تحت تراكيز مختلفة من الحديد يمكن استنتاج أن التركيز 0.03 ملي مول من الحديد عند 20 ساعة فترة حضانة هي الظروف المثالية لنمو الوزن الطري للفطر مما أثر إيجابيا وأدى إلى زيادة إنتاج حاملات الحديد. من التحليل الكيميائي، وجد أن الصيغة الكيميائية $C_{39}H_{58}FeN_6O_{15}$ كانت متوافقة مع حامل الحديد المعروف ترايستيل فيوزارنين سى.